ELSEVIER

Materials Chemistry and Physics 40 (1995) 30–36

MATERIALS CHEMISTRY AND PHYSICS

Optical properties of $As_{50}Se_{50}$ semiconducting glass films of non-uniform thickness deposited by thermal evaporation

J.B. Ramírez-Malo, C. Corrales, E. Márquez, J. Reyes, J. Fernández-Peña, P. Villares, R. Jiménez-Garay

Departamento de Estructura y Propiedades de los Materiales, Facultad de Ciencias, Universidad de Cádiz, Ap. 40, 11510 Puerto Real (Cádiz), Spain

Received 4 May 1994; accepted 12 October 1994

Abstract

Based on the interference fringes in optical transmission spectra at normal incidence of wedge-shaped thin films of $As_{50}Se_{50}$ semiconducting glass, deposited by thermal evaporation, an optical method is applied that makes it possible to obtain a parameter indicating the degree of film thickness uniformity, and to accurately determine the refractive index, subsequently used to derive the average film thickness. Thickness measurements have been performed with a surface-profiling stylus to cross-check the results from the transmission spectra, and excellent agreement was found between the two types of measurements. The dispersion of the refractive index is discussed in terms of the single-oscillator Wemple–DiDomenico model, and the optical absorption edge is described using the 'non-direct transition' model proposed by Tauc. Likewise, the optical energy gap is derived from Tauc's extrapolation.

Keywords: Arsenic; Selenium; Semiconducting glass films

1. Introduction

Over the last two decades, interest in the knowledge of the properties of chalcogenide glasses has grown considerably, owing to the wide range of phenomena exhibited by these semiconducting materials when samples in a suitable form are exposed to light or other irradiation. At least seven distinct photo-induced structural or physico-chemical changes have been observed in amorphous chalcogenides, viz., photo-crystallization, photo-polymerization, photo-decomposition (in compounds), photo-induced morphological changes, photo-vaporization, photo-dissolution (of certain metals, particularly silver), and light-induced changes in the local atomic configuration [1,2]. In general, these phenomena are accompanied by changes in the optical constants of the material and in particular shifts in the absorption edge, i.e., photo-darkening or photo-bleaching. The accurate determination of the optical constants of these glassy materials is a prerequisite not only for a full understanding of the basic mechanism of the photo-induced phenomena, but also for exploiting its technological potentials.

Among the existing methods for determining the optical constants, those based exclusively on the optical transmission spectra at normal incidence [3,4] have been applied to different crystalline and amorphous materials deposited on transparent substrates in the form of thin films, following different techniques [5–7]. These relatively simple methods, besides being non-destructive and no requiring any previous knowledge of the thickness of the deposited film, are fairly accurate, as the thickness and refractive index can be determined with an accuracy of about 1% [4]. They do, however, assume a film with uniform thickness which, when absent, produces a shrinking in the optical transmission spectrum, leading to less accurate final results and even serious errors.

The aim of this work is to apply the Swanepoel method [8] to non-uniform films and to obtain from the transmission spectrum at normal incidence a parameter indicating the degree of uniformity of the film thickness, and an excellent accuracy in the determination of the optical constants of the thin film despite the aforementioned deformations in the transmission spectrum. The very appealing procedures that have been

0254-0584/95/$09.50 © 1995 Elsevier Science S.A. All rights reserved
SSDI 0254-0584(94)01451-L

applied by Swanepoel for the optical characterization of non-uniform films of a-Si and a-Si:H, and by the authors of the present work for thin films of Ag-photodoped $As_{30}S_{70}$ glass [9], are here applied to wedge-shaped thin films corresponding to the chemical composition $As_{50}Se_{50}$, especially interesting because of a recently discovered photo-induced effect, namely the athermal photo-induced vitrification [10,11].

2. Experimental

Thin-film samples were prepared by vacuum evaporation of powdered melt-quenched glassy material onto clean glass substrates. The thermal evaporation process was carried out in a coating system (Edwards, model E306A) at a pressure of $\approx 5\times10^{-7}$ torr from a suitable quartz crucible. During the deposition process, the temperature rise of the substrate due to radiant heating from the crucible was negligible. The deposition rate was $\approx$5–10 Å s^{-1}, which was measured continuously by a quartz crystal monitor (Edwards, model FTM-5). It is well known that such a low deposition rate produces a film composition very close to that of the bulk starting material (electron microprobe analysis has indicated that the film stoichiometry is correct to ±1 at.%). The lack of crystallinity in the whole films was verified by X-ray diffraction analysis. Fig. 1 shows a typical X-ray diffraction pattern (using the Cu Kα line) for as-deposited glass films, where we may see the first sharp diffraction peak at a value of $2\theta\approx17°$, which is associated with the medium-range order of the structure [12,13].

The optical transmission spectra were obtained over the spectral region 0.4–2.5 μm by a double-beam UV/Vis/NIR computer-controlled spectrophotometer (Perkin-Elmer, model Lambda-19). The area of illumination over which a single transmission spectrum was obtained is about 1×10 mm. It should be emphasized that the transmission spectra clearly show that the a-$As_{50}Se_{50}$ films have non-uniform thickness. This was confirmed by measurements of the film thickness by a stylus-based surface profiler (Sloan, model Dektak IIA). All the measurements of optical constants reported in this paper were made at room temperature.

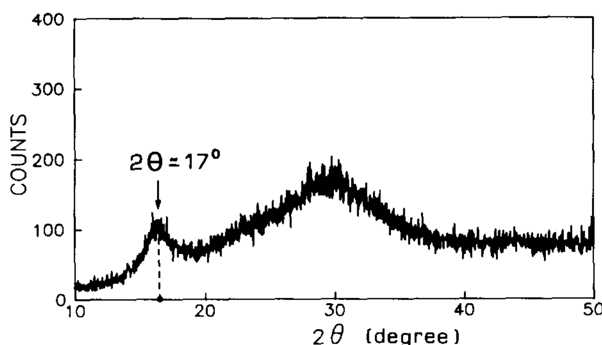

Fig. 1. X-ray diffraction pattern (Cu Kα radiation) of an as-evaporated $As_{50}Se_{50}$ glass film.

3. Theoretical considerations

In the present paper we assume a thin film of non-uniform thickness deposited on a transparent substrate with refractive index s. The system is surrounded by air with refractive index $n_0=1$. The film has a complex refractive index $n_c=n-ik$ and an absorption coefficient α. The extinction coefficient k is related to α by $k=\alpha\lambda/4\pi$. If the thickness variation of the film (see Fig. 2) is assumed to be linear over the area irradiated by the spectrophotometer, then the thickness d may be expressed as a function of the average thickness $\bar{d}$, by $d=\bar{d}+\eta\Delta d$, with $-1\leqslant\eta\leqslant1$; the parameter Δd measures the actual deviation from the average thickness $\bar{d}$, as can be seen in Fig. 2, at the extremes of the irradiated area.

In the case of a film with uniform thickness the transmission $T(\lambda, s, n, d, k)$ is expressed by a complex expression [14,15] which can be simplified given that $n^2\gg k^2$, which is practically valid for the entire spectral range, and results in

$$T=\frac{Ax}{B-Cx\cos\varphi+Dx^2} \tag{1}$$

where $A=16n^2s$; $B=(n+1)^3(n+s^2)$; $C=2(n^2-1)\times(n-s^2)$; $D=(n-1)^3(n-s^2)$; $\varphi=4\pi nd/\lambda$; and $x=\exp(-\alpha d)$. On the other hand, in the spectral region of transparency $x=1$, and Eq. (1) is transformed to

$$T=\frac{A}{B-C\cos\varphi+D} \tag{2}$$

In addition, the optical transmission at a specific wavelength λ in the case of non-uniform thickness with the above-mentioned characteristics can be obtained by integrating Eq. (2):

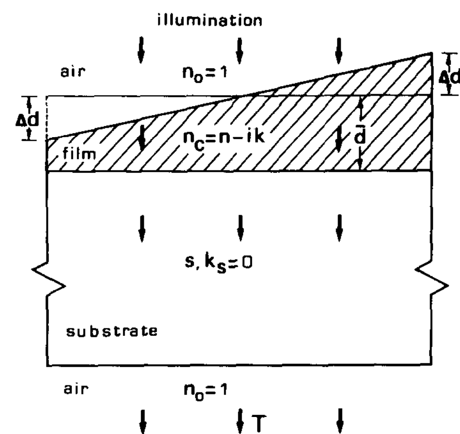

Fig. 2. Diagram showing an absorbing thin film with a linear variation in thickness on a thick transparent substrate.

$$T(\lambda)=\frac{1}{\varphi_2-\varphi_1}\int_{\varphi_1}^{\varphi_2}\frac{A}{B-C\cos\varphi+D}\,d\varphi \qquad (3)$$

where $\varphi_1=4\pi n(\bar{d}-\Delta d)/\lambda$ and $\varphi_2=4\pi n(\bar{d}+\Delta d)/\lambda$. This integration leads to

$$T(\lambda)=\frac{\lambda}{4\pi n\Delta d}\frac{a}{(1-b^2)^{1/2}}\left[\tan^{-1}\left(\frac{1+b}{(1-b^2)^{1/2}}\tan\frac{\varphi_2}{2}\right)-\tan^{-1}\left(\frac{1+b}{(1-b^2)^{1/2}}\tan\frac{\varphi_1}{2}\right)\right] \qquad (4)$$

where $a=A/(B+D)$ and $b=C/(B+D)$.

3.1. Determining the refractive index and average film thickness

Following the Swanepoel method [8], the envelopes around the maxima and minima of the spectrum are considered to be continuous functions of λ and, thus, of $n(\lambda)$. From Eq. (2) it follows that at a maximum

$$\frac{2\pi n\bar{d}}{\lambda}=l\pi \qquad l=0, 1, 2, 3, \ldots$$

which yields

$$\tan\frac{\varphi_2}{2}=\tan\left(\frac{2\pi n\Delta d}{\lambda}\right) \qquad (5)$$

$$\tan\frac{\varphi_1}{2}=-\tan\left(\frac{2\pi n\Delta d}{\lambda}\right) \qquad (6)$$

Substituting Eqs. (5) and (6) in Eq. (4), the expressions for the envelopes around the maxima and minima are obtained:

$$T_{Md}(\lambda),\, T_{md}(\lambda)=\frac{\lambda}{2\pi n\Delta d}\frac{a}{(1-b^2)^{1/2}}\times\tan^{-1}\left[\frac{1\pm b}{(1-b^2)^{1/2}}\tan\left(\frac{2\pi n\Delta d}{\lambda}\right)\right] \qquad (7),(8)$$

where + in the $\pm$ refers to $T_{Md}(\lambda)$ and − to $T_{md}(\lambda)$. The validity range of Eqs. (7) and (8) is $0<\Delta d<\lambda/4n$. Based on the interference extremes present in the transmission spectrum, both envelopes were generated by computer using a very useful program specifically designed to calculate the envelopes of the optical interference spectrum [16].

On the other hand, the necessary values of the refractive index of the substrate for each interference extreme are obtained from the transmission spectrum of the substrate alone, T_s, using the well-known expression

$$s=\frac{1}{T_s}+\left(\frac{1}{T_s^2}-1\right)^{1/2}$$

For each specific wavelength, Eqs. (7) and (8) form a system with the unknown parameters n and Δd. Within the aforementioned validity range the system has only one solution [17].

Continuing with the theoretical considerations, in the region of weak and medium absorption ($\alpha>0$), the integration (1) should be done over both the film thickness variation and absorptance. This is prohibitively difficult analytically, and an approximation would be to consider x to have an average value over the range of integration with respect to Δd. This is an excellent approximation provided $\Delta d\ll\bar{d}$. The constants a and b are now redefined as follows: $a_x=Ax/(B+Dx^2)$, $b_x=Cx/(B+Dx^2)$, with $x=\exp(-\alpha\bar{d})$. The equations for the two envelopes now become

$$T_{Mx}(\lambda),\, T_{mx}(\lambda)=\frac{\lambda}{2\pi n\Delta d}\frac{a_x}{(1-b_x^2)^{1/2}}\times\tan^{-1}\left[\frac{1\pm b_x}{(1-b_x^2)^{1/2}}\tan\left(\frac{2\pi n\Delta d}{\lambda}\right)\right] \qquad (9),(10)$$

where again + in the $\pm$ refers to $T_{Mx}(\lambda)$ and − to $T_{mx}(\lambda)$. These expressions are again two independent transcendental equations with two unknown parameters, n and x, since Δd is known from solving Eqs. (7) and (8) in the transparent region. Eqs. (9) and (10) have again one unique solution for n and x in the range $0<x\leqslant 1$. The procedure to be used to calculate the absorption coefficient α will be shown in the next section. Once the system that results from each interference extreme is resolved, the corresponding refractive index is obtained. From these, one can determine the average thickness $\bar{d}$, and also apply a procedure, similar to the one for uniform films [7,18,19], to increase the accuracy using the basic interference equation

$$2n\bar{d}=m\lambda \qquad (11)$$

where m is the interference order, integer or half-integer, for a maximum and a minimum, respectively. Applying Eq. (11) to each pair of consecutive maxima and minima, the interference orders m_0 are estimated, which, once rounded off to the nearest corresponding integer or half-integer, yield refractive index and final average thickness values with an accuracy of better than 2%. The subsequent fitting of these refractive index values to a specific dispersion model, described below, permits the extrapolation of the refractive index towards the spectral range with no interference effects.

3.2. Determining the absorption coefficient and optical band gap

In the case of a film with uniform thickness, the absorptance x can be obtained from the envelope around the maxima [8] by

$$x=\frac{E_M-[E_M{}^2-(n^2-1)^3(n^2-s^4)]^{1/2}}{(n-1)^3(n-s^2)} \tag{12}$$

where

$$E_M=\frac{8n^2s}{T_M}+(n^2-1)(n^2-s^2)$$

These formulae are also valid for non-uniform films in the spectral region where there are no interference fringes, and therefore the envelopes converge to a single curve, $T_M=T_m$. However, once the transmission is affected by the interferences, i.e., when $T_M \neq T_m$, the shrinking of the spectrum influences the values of T_M and hence the absorptance calculated by Eq. (12). Below we will explain how α calculated by Eq. (12) is affected by the shrinking of the transmission spectrum. Since the absorptance and the average thickness $\bar{d}$ are known, the relation $x=\exp(-\alpha\bar{d})$ can be solved for α, thus yielding the absorption coefficient. Moreover, from the relationship $k=\alpha\lambda/4\pi$, the extinction coefficient is obtained.

Finally, the optical gap is determined from the calculated values of α. The absorption coefficient of amorphous semiconductors in the high-absorption region ($\alpha > \approx 10^4$ cm^{-1}), assuming parabolic band edges and energy-independent matrix elements for interband transitions, is given according to the nondirect transition for the direct gap model proposed by Tauc [20] by the following equation:

$$\alpha(h\nu)=K_1\frac{(h\nu-E_g^{opt})^2}{h\nu} \tag{13}$$

where $h\nu$, E_g^{opt} and K_1, denote the photon energy, optical energy gap and an energy-independent constant, respectively. Formally, the optical gap E_g^{opt} is obtained as the intercept of the plot of $(\alpha h\nu)^{1/2}$ against $h\nu$.

4. Results and discussion

Fig. 3 presents a typical optical transmission spectrum for a thin film of $As_{50}Se_{50}$ semiconducting glass, together with that of the substrate alone. The envelopes of the transmission spectrum can be observed, along with the points corresponding to each interference extreme. On the other hand, for each interference maximum and minimum one obtains the sets of values $[\lambda_i, T_M(\lambda_i), T_m^*(\lambda_i)]$ and $[\lambda_j, T_M^*(\lambda_j), T_m(\lambda_j)]$, respectively, which define the systems of the two equations (7) and (8). The values $T_m^*(\lambda_i)$ and $T_M^*(\lambda_j)$ – the calculated points in Fig. 3 – are those associated to the envelopes and are shown in Table 1. These equations are resolved using an iterative algorithm based on a Newtonian method, and the refractive index and uniformity parameter values obtained by resolving each system are

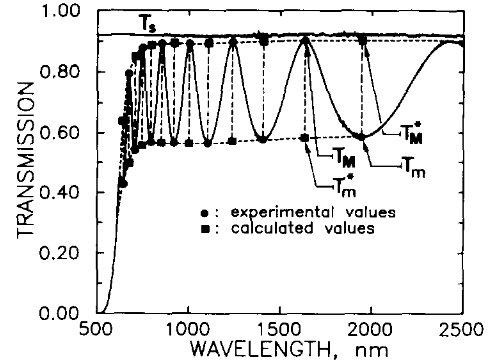

Fig. 3. An optical transmission spectrum of a wedge-shaped $As_{50}Se_{50}$ glass film of 933 nm average thickness on a glass substrate. Curves T_M and T_m are the maximum and minimum envelopes. T_s is the transmission spectrum of the substrate alone.

shown in columns n_2 and Δd, respectively, of Table 1. The n_1 refractive indices in this table show the values that would be obtained if the transmission spectra of non-uniform films were treated with the method for uniform films [7,18,19]. From the values obtained for the parameter Δd, it seems reasonable to suggest a value for the thickness variation of ≈ 22 nm. The values of Δd, T_M and T_m are now used in Eqs. (9) and (10) to calculate the refractive index and absorptance, listed as n_3 and x in Table 1. It can be seen that the n_3 values are 2% to 7% greater than the corresponding n_1 value, in the case of a film with uniform thickness. The accuracy of the refractive indices n_3 is even further improved by Eq. (11), through the procedure described above, which is shown in Table 2, where the final refractive indices are listed in the n_4 column. In addition, the final average thickness was determined and the value turned out to be 933 ± 10 nm, showing an excellent agreement between this thickness and that determined by mechanical measurements in the same area of the film, which is 923 ± 18 nm.

Furthermore, the refractive index dispersion can be fitted to the Wemple–DiDomenico relation [21]

$$\epsilon_1(E)=n^2(E)=1+\frac{E_0E_d}{E_0{}^2-E^2} \tag{14}$$

where E_0 is the energy of the effective dispersion oscillator (typically near the main peak of the $\epsilon_2(E)$ spectrum), which is identified by the mean transition energy from the valence band of the lone-pair state to the conduction-band state (in these chalcogenide materials, the valence s states lie far below the top of the valence band and the band edge involves transitions between lone-pair p states and antibonding conduction-band states [21]), and E_d is the dispersion energy. This latter, very important quantity obeys the empirical relationship $E_d=\beta N_c Z_a N_e$, where $\beta=0.37\pm0.04$ eV, N_c is the number of nearest-neighbour cations to the anion, Z_a is the formal chemical valency of the anion,

Table 1
Values of various parameters for $As_{50}Se_{50}$ films [a]

λ (nm)	s	T_M	T_m	n_1	n_2	Δd (nm)	n_3	x
1943	1.512	0.904	0.586	2.520	2.611	36.4	2.578	1.000
1631	1.506	0.904	0.582	2.538	2.623	31.6	2.592	1.000
1406	1.533	0.900	0.577	2.553	2.656	24.6	2.644	1.000
1236	1.531	0.896	0.569	2.565	2.692	23.9	2.678	1.000
1106	1.540	0.893	0.564	2.582	2.717	21.6	2.713	1.000
1002	1.534	0.892	0.564	2.599	2.718	20.9	2.719	1.000
919	1.542	0.892	0.564	2.622	2.721	18.3	2.743	1.000
851	1.519	0.892	0.566	2.649	2.707	19.0	2.727	1.000
794	1.521	0.888	0.567	2.677	2.710	18.9	2.734	1.000
746	1.522	0.879	0.559	2.709	2.754	19.5	2.776	0.999
706	1.519	0.849	0.542	2.747	2.867	23.3	2.816	0.986
673	1.517	0.795	0.500	2.793	3.137	25.7	2.955	0.951
643	1.521	0.638	0.430	2.835	3.885	28.7	3.017	0.807

[a] The non-underlined values for T_M and T_m correspond to the experimental interference maximum and minimum, respectively, whereas the underlined values are those calculated by the envelope computer program (see Fig. 2). The n_1 column shows the refractive indices obtained assuming a film of uniform thickness; n_2 and Δd are the solutions of Eqs. (7) and (8), and n_3 and x are the solutions of Eqs. (9) and (10), for each specific wavelength.

Table 2
Accuracy improvement procedure for refractive indices n_3 and determination of the average film thickness from Eq. (11)

λ (nm)	n_3	$\bar{d}_1$ (nm)	m_0	m	$\bar{d}_2$ (nm)	n_4
1943	2.578	–	2.51	2.5	942	2.604
1631	2.592	–	3.00	3.0	944	2.623
1406	2.644	904	3.55	3.5	931	2.638
1236	2.678	865	4.09	4.0	923	2.650
1106	2.713	872	4.63	4.5	917	2.668
1002	2.719	915	5.12	5.0	921	2.686
919	2.743	940	5.64	5.5	921	2.709
851	2.727	1019	6.05	6.0	936	2.737
794	2.734	1090	6.50	6.5	944	2.767
746	2.776	969	7.03	7.0	941	2.799
706	2.816	918	7.53	7.5	940	2.838

$\bar{d}_1=944$ nm, $\sigma_1=73$ nm (7.7%); $\bar{d}_2=933$ nm, $\sigma_2=10$ nm (1.1%)

and N_e is the effective number of valence electrons per anion. By plotting $(n^2-1)^{-1}$ against E^2 and fitting a straight line as shown in Fig. 4, E_0 and E_d can be determined directly from the intercept on the vertical axis, E_0/E_d, and the slope $(E_0E_d)^{-1}$. The equation for the straight line belonging to the least-squares fit is $(n^2-1)^{-1}=0.177-0.011E^2$, with a correlation coefficient of 0.995. The values obtained for the dispersion parameters E_0 and E_d, derived from the above-mentioned equation, are $E_0=3.98$ eV and $E_d=22.44$ eV. On the other hand, from this value of E_d, and considering that for this particular glass composition, $Z_a=2$ and $N_c=11$, then $N_c\approx 2.8$. The Wemple–DiDomenico dispersion curve is also shown in Fig. 4, together with the corresponding refractive-index data.

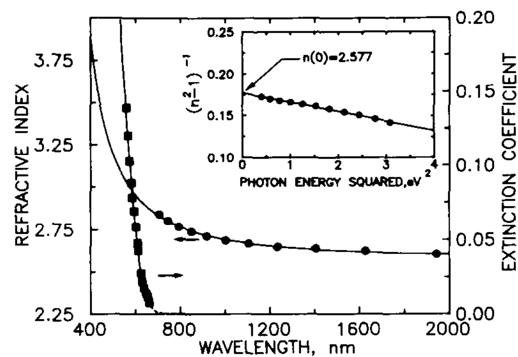

Fig. 4. Refractive index and extinction coefficient vs. wavelength. The inset is a plot of the refractive-index factor $(n^2-1)^{-1}$ vs. E^2 (the $n(0)$ value is the refractive index extrapolated to $E=0$).

The optical absorption spectrum obtained using Eq. (12) is displayed in Fig. 5. In the high-absorption region, according to Eq. (13), a value of $K_1=5.2\times10^5$ eV^{-1} cm^{-1} is obtained – this constant K_1 is almost independent of the chemical composition of the chalcogenide semiconductor films [22]. In the weak-absorption region (1 cm$^{-1}<\approx\alpha<\approx10^4$ cm^{-1}), the absorption depends exponentially on the photon energy (Urbach relation) [17]:

$$\alpha=\alpha_0\exp\left(\frac{h\nu}{K_2}\right) \tag{15}$$

where K_2 is a slope parameter. This part of the absorption spectrum corresponds to electronic transitions between tail-states and band-states. The value of K_2 obtained is approximately 0.06 eV. On the other hand, to account for the influence of the shrinking of the transmission spectrum in the interference region on

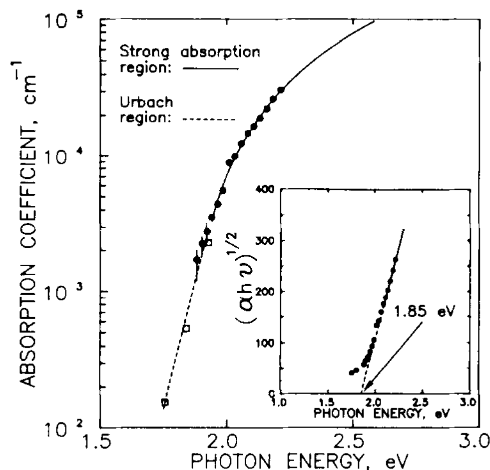

Fig. 5. Optical-absorption edge for the glass composition $As_{50}Se_{50}$ and, in the inset, the associated Tauc extrapolation.

the values of α, we take the realistic absolute change of $T_M \pm 0.01$. Some α values calculated from x values listed in the last column of the Table 1, which are smoothly connected with those obtained by Eq. (12), are also plotted. Fig. 4 also shows the spectrum corresponding to the extinction coefficient where the absorption edge can clearly be seen.

Together with the spectrum corresponding to the absorption coefficient, Fig. 5 shows the Tauc plot, which makes it possible to calculate the optical energy gap, yielding a value of 1.85 eV, slightly over the value determined for the stoichiometric composition As_2Se_3 of 1.80 eV [23]. This result agrees with the compositional trend of E_g^{opt} found in the As–Se glass system [24]: the optical band gap shows a minimum value for an As content of about 42 at.% (obviously, very near the stoichiometric composition As_2Se_3). Yamaguchi's approach [22] relates the stoichiometry of the compound and the value of its optical bandgap: if there is a linear relationship between the bond strengths and the average bandgap, and if one allows their superposition to describe the compounds, then the addition of As–As or Se–Se bonds to the stoichiometric compound containing only As–Se bonds will affect the average bandgap. However, since the strengths of the As–As, As–Se and Se–Se bonds are very similar, 1.88, 2.10 and 1.89 eV, respectively, the small minimum in E_g^{opt} for the stoichiometric compound cannot be explained from the point of view of bond energy. When the bond energies in the glass system are not very different, this behaviour can be explained by assuming that the increase in disorder associated with deviations from stoichiometry would tend to push the mobility edges further into the bands, thereby increasing E_g^{opt} [25]. There may also be additional factors, such as compositional heterogeneities, that may add to the shift of the absorption edge. Finally, the ratio E_0/E_g^{opt} takes the value 2.15 (Tanaka obtained a value of ≈ 1.90 for the annealed As–S semiconducting glasses [26]).

5. Conclusions

The procedures reported in this paper for calculating the thickness and optical constants of thermally evaporated $As_{50}Se_{50}$ thin films have successfully been applied to layers whose film thickness ranges between around 700 and 1200 nm. The lack of uniformity of the film thickness found under the present preparation conditions gives rise to a clear shrinking of the interference fringes of the optical transmission spectrum at normal incidence; inaccuracies and even serious errors occur if n, d and α are calculated from such a transmission spectrum assuming the film to be uniform. The optical method applied here makes it possible to determine the refractive index and average thickness with an accuracy of better than $\pm 2\%$. The average thickness and thickness variation were cross-checked with those determined using the mechanical stylus instrument; there was very good agreement between the two types of measurements. The subsequent fitting of the refractive index to the Wemple–DiDomenico relationship results in dispersion parameters directly related to the structure of the glassy material under study. Worth noting, finally, is the particular interest of the optical characterization of thin films of glassy composition $As_{50}Se_{50}$, as it shows one of the latest photo-induced phenomena in chalcogenide materials, namely the athermal photo-vitrification process. This phenomenon can briefly be described as follows: X-ray diffraction patterns show that the exposure of the previously crystallized $As_{50}Se_{50}$ thin films to white light for ≈ 10 h at room temperature causes the complete disappearance of the crystalline features subsequent to thermal annealing at ≈ 150 °C for 24 h. The authors are currently testing the application of this optical method to the study of the changes undergone by the optical constants of the film when subjected to successive crystallization-on-annealing and vitrification-on-illumination processes.

References

[1] A.E. Owen, A.P. Firth and P.J.S. Ewen, *Philos. Mag. B, 52* (1985) 347.

[2] P.J.S. Ewen and A.E. Owen, in M. Cable and J.M. Parker (eds.), *High-performance Glasses,* Blackie, London, 1992.

[3] J.C. Manifacier, J. Gasiot and J.P. Fillard, *J. Phys. E: Sci. Instrum., 9* (1976) 1002.

[4] R. Swanepoel, *J. Phys. E: Sci. Instrum., 16* (1983) 1214.

[5] M. Hamman, M.A. Harith and W.H. Osman, *Solid State Commun., 59* (1986) 271.

[6] J.A. Kalomiros and J. Spyridelis, *Phys. Status Solidi (a), 107* (1988) 633.

[7] E. Márquez, J. Ramírez-Malo, P. Villares, R. Jiménez-Garay, P.J.S. Ewen and A.E. Owen, *J. Phys. D: Appl. Phys., 25* (1992) 535.
[8] R. Swanepoel, *J. Phys. E: Sci. Instrum., 17* (1984) 896.
[9] E. Márquez, J.B. Ramírez-Malo, J. Fernández-Peña, R. Jiménez-Garay, P.J.S. Ewen and A.E. Owen, *Opt. Mater., 2* (1993) 143.
[10] S.R. Elliott and A.V. Kolobov, *J. Non-Cryst. Solids, 128* (1991) 216.
[11] A.V. Kolobov, V.A. Bershtein and S.R. Elliott, *J. Non-Cryst. Solids, 150* (1992) 116.
[12] O.V. Luksha, V.I. Mikla, V.P. Ivanitsky, A.V. Mateleshko and D.G. Semak, *J. Non-Cryst. Solids, 144* (1992) 253.
[13] S.R. Elliott, *J. Non-Cryst. Solids, 106* (1988) 26.
[14] O.S. Heavens, *Optical Properties of Thin Solid Films,* Butterworths, London, 1955.
[15] A. Mini, *Ph.D. Thesis,* L'Université Scientifique et Médicale de Grenoble, 1982.
[16] M. McClain, A. Feldman, D. Kahaner and X. Ying, *Computers Phys., 5* (1990) 45.
[17] J.I. Cisneros, G.B. Rego, M. Tomyiama, S. Bilac, J.M. Goncalves, A.E. Rodrigues and Z.P. Argüello, *Thin Solid Films, 100* (1983) 155.
[18] J.B. Ramírez-Malo, E. Márquez, P. Villares and R. Jiménez-Garay, *Phys. Status Solidi (a), 133* (1992) 499.
[19] J.B. Ramírez-Malo, E. Márquez, P. Villares and R. Jiménez-Garay, *Mater. Lett., 17* (1993) 327.
[20] J. Tauc, *J. Non-Cryst. Solids, 8–10* (1972) 569.
[21] S.H. Wemple, *Phys. Rev. B, 8* (1973) 3767.
[22] M. Yamaguchi, *Philos. Mag. B, 51* (1985) 651.
[23] J.B. Ramírez-Malo, E. Márquez, C. Corrales, P. Villares and R. Jiménez-Garay, *Mater. Sci. Eng. B, 25* (1994) 53.
[24] K. Shimakawa, *J. Non-Cryst. Solids, 43* (1981) 229.
[25] C.H. Hurst and E.A. Davis, *J. Non-Cryst. Solids, 16* (1974) 343.
[26] K. Tanaka, *Thin Solid Films, 66* (1980) 271.